

Na/K-ATPase Mimetic pNaKtide Peptide Inhibits the Growth of Human Cancer Cells^{*,§}

Received for publication, November 29, 2010, and in revised form, July 21, 2011. Published, JBC Papers in Press, July 22, 2011, DOI 10.1074/jbc.M110.207597

Zhichuan Li^{‡§}, Zhongbing Zhang[‡], Joe X. Xie[‡], Xin Li[¶], Jiang Tian^{‡§}, Ting Cai[‡], Hongjuan Cui^{||1}, Hanfei Ding^{||2}, Joseph I. Shapiro[§], and Zijian Xie^{‡§3}

From the Departments of [‡]Physiology and Pharmacology, [¶]Pathology, ^{||}Biochemistry and Cancer Biology, and [§]Medicine, University of Toledo College of Medicine, Toledo, Ohio 43614

Cells contain a large pool of nonpumping Na/K-ATPase that participates in signal transduction. Here, we show that the expression of $\alpha 1$ Na/K-ATPase is significantly reduced in human prostate carcinoma as well as in several human cancer cell lines. This down-regulation impairs the ability of Na/K-ATPase to regulate Src-related signaling processes. A supplement of pNaKtide, a peptide derived from $\alpha 1$ Na/K-ATPase, reduces the activities of Src and Src effectors. Consequently, these treatments stimulate apoptosis and inhibit growth in cultures of human cancer cells. Moreover, administration of pNaKtide inhibits angiogenesis and growth of tumor xenograft. Thus, the new findings demonstrate the *in vivo* effectiveness of pNaKtide and suggest that the defect in Na/K-ATPase-mediated signal transduction may be targeted for developing new anticancer therapeutics.

Na/K-ATPase was originally discovered as an ion pump that is essential for cell vitality and provides a means for epithelium to secrete and/or absorb solutes and nutrients (1, 2). Recent studies have revealed that in addition to pumping ions across the cell membrane, Na/K-ATPase, specifically the $\alpha 1$ isoform, conducts many nonpumping functions, including scaffolding and signal transduction. As a signaling protein, it is involved in the formation of membrane structures such as tight junction and caveolae (3, 4). Moreover, a large fraction of cellular Na/K-ATPase is involved in tethering and regulating multiple protein and lipid kinases as well as membrane receptors (e.g. Src, human epidermal growth factor receptor, and PI3K) in a cell-specific manner (5, 6). Recently, the $\alpha 1$ Na/K-ATPase–Src receptor complex has been identified as one of the central components of $\alpha 1$ Na/K-ATPase-mediated signaling transduction (7). In this receptor complex, the Src SH2 domain binds to the second cytosolic domain, whereas the Src kinase domain inter-

acts with the nucleotide binding (N) domain⁴ of the $\alpha 1$ subunit. The latter interaction keeps Src in an inactive state (7). It is important to note that normal epithelial cells express approximately one million $\alpha 1$ Na/K-ATPase molecules (roughly five times the amount of Src). Thus, $\alpha 1$ Na/K-ATPase could provide at least two ways of regulating cellular Src activity. First, it could bind and keep Src in an inactive state. Consistently, when knock-out of one copy of the $\alpha 1$ gene caused a 20–30% reduction in cellular $\alpha 1$ Na/K-ATPase, it produced a >2-fold increase in Src and ERK activities in tissues of $\alpha 1^{+/-}$ mice (8). Second, formation of the Na/K-ATPase–Src complex provides a functional receptor for endogenous cardiotonic steroids such as ouabain to regulate cellular signaling via Src and Src effectors (7, 9). Thus, changes in cellular $\alpha 1$ Na/K-ATPase would have a significant effect on cellular signaling events induced by either cardiotonic steroids or other growth factors through Src-related pathways.

Based on the fact that the N domain of the $\alpha 1$ subunit binds and inhibits Src, we have recently made pNaKtide from the N domain of the human $\alpha 1$ subunit of Na/K-ATPase (10). Addition of TAT leader sequence makes it cell-permeable. Moreover, a majority of pNaKtide appears to be localized in the plasma membrane in cultured cells. Like the N domain of $\alpha 1$ Na/K-ATPase, pNaKtide binds and inhibits the Na/K-ATPase-interacting pool of Src (10). Consistently, pNaKtide blocks the formation of the receptor Na/K-ATPase–Src complex but does not alter the basal cellular Src activity in cells where $\alpha 1$ Na/K-ATPase is adequately expressed (10). Thus, pNaKtide functions like a receptor antagonist, capable of inhibiting ouabain-induced signal transduction (10). On the other hand, it also works like $\alpha 1$ Na/K-ATPase (11) and is capable of inhibiting Src and Src effectors in cells where the expression of Na/K-ATPase is reduced (10).

Src regulates cell proliferation/apoptosis, migration, and invasion (12, 13) and is involved in the progression of many types of cancers (14). Once activated by either receptors (e.g. human epidermal growth factor receptor and androgen receptors) or membrane receptor-associated proteins (e.g. G proteins) (15–17), Src is recruited to the cell periphery, focal adhesion, and tight junction where the $\alpha 1$ Na/K-ATPase resides in a high concentration (18–20). Previously, we have shown that

* This work was supported, in whole or in part, by National Institutes of Health Grants HL-36573 from the NHLBI and GM-78565 from the NIGMS.

§ The on-line version of this article (available at <http://www.jbc.org>) contains supplemental Figs. S1 and S2.

¹ Present address: State Key Laboratory of Silkworm Genome Biology, Institute of Sericulture and Systems Biology, Southwest University, Chongqing 400715, China.

² Present address: Dept. of Pathology, Medical College of Georgia, Augusta, GA 30912.

³ To whom correspondence should be addressed: Dept. of Physiology and Pharmacology, Mail Stop 1008, University of Toledo College of Medicine, 3000 Arlington Ave., Toledo, OH 43614. Tel.: 419-383-4182; Fax: 419-383-2871; E-mail: Zi-Jian.Xie@utoledo.edu.

⁴ The abbreviations used are: N domain, nucleotide binding domain; FAK, focal adhesion kinase; IHC, immunohistochemical; MTT, 3-(4,5-dimethylthiazol-2-yl)-2,5-diphenyltetrazolium bromide; PARP, poly(ADP-ribose) polymerase; PI, propidium iodide; TCEP, Tris(2-carboxyethyl)phosphine.

epithelial cells actually contain two functionally distinct pools of Na/K-ATPase and that reduction of cellular $\alpha 1$ Na/K-ATPase preferentially depletes the Src-interacting pool of Na/K-ATPase, resulting in an elevation in cellular activities of Src and Src effectors (8, 11, 21). Thus, should $\alpha 1$ Na/K-ATPase be down-regulated in cancer cells, this could contribute to an increase in kinase activity observed in cancers such as prostate carcinoma. Conversely, repletion of $\alpha 1$ Na/K-ATPase or application of pNaKtide would antagonize the increase in kinase activity, which could inhibit tumor growth. To test these hypotheses, we first assessed the expression of $\alpha 1$ Na/K-ATPase in prostate carcinomas and established cancer cell lines and measured the Na/K-ATPase-mediated signal transduction focusing on those that are Src-related. We then tested whether application of $\alpha 1$ Na/K-ATPase mimetics such as pNaKtide could attenuate the activities of cellular Src and Src effectors and inhibit tumor growth.

EXPERIMENTAL PROCEDURES

Materials—Staurosporine was obtained from Calbiochem. The following antibodies were obtained from Santa Cruz Biotechnology: Src (sc-8056), poly(ADP-ribose) polymerase (PARP-1; sc-8007), c-Myc (sc-40), ERK (sc-94), phospho-ERK (sc-7383), and GAPDH (sc-20357). Antibodies against phospho-focal adhesion kinase (FAK) (Tyr-576/Tyr-577) (3281) and FAK (3285) were from Cell Signaling Technology. Antibodies against VEGF (Abcam, ab46154) and phosphotyrosine 418 (Invitrogen, 44-660G) were also used. HRP-conjugated anti-rabbit and anti-mouse secondary antibodies were obtained from Santa Cruz Biotechnology. The monoclonal anti- $\alpha 1$ antibody $\alpha 6f$ was obtained from the Developmental Studies Hybridoma Bank at the University of Iowa. pNaKtide was synthesized with purity above 95%. All other chemicals were from Sigma-Aldrich.

Cell Culture—RWPE-1, DU145, LNCaP, PC-3, and LLC-PK1 cells were all from American Type Culture Collection (ATCC) and grown according to ATCC recommendations. DU145 and PC-3 are prostate cancer cell lines originally isolated from metastatic sites in brain and bone, respectively. LNCaP cells recapitulate prostate cancer progression due to relatively slow growth and expression of androgen receptor, whereas RWPE-1 is a nontumorigenic human prostate epithelial cell line. Human umbilical vein endothelial cells and human aortic endothelial cells were obtained from Lonza (Walkersville, MD) and maintained in the M199 medium supplemented with 10% FBS, 50 μ g/ml endothelial cell growth supplement (BD Biosciences), and 50 μ g/ml heparin (BD Biosciences). The Na/K-ATPase $\alpha 1$ -knockdown TCN23-19 cells were developed from LLC-PK1 cells and maintained as described (11).

Plasmid Constructs and Transient Transfections—The CMV promoter-driven pEYFP-ND1 construct was generated as described (10). Transient transfections were performed using Lipofectamine 2000 (Invitrogen) according to the manufacturer's instructions. Expression of YFP or YFP-tagged proteins was monitored using an Olympus fluorescence microscope. Images were processed with SPOT software version 4.60 (Diagnostic Instruments).

Immunoblot Analysis—Immunoblot analysis was performed as described previously (22). Following the indicated treatment, the cells were washed rapidly with ice-cold PBS. Then the cells were lysed in modified ice-cold radioimmune precipitation assay buffer containing 1% Nonidet P-40, 1% sodium deoxycholate, 150 mM NaCl, 1 mM EDTA, 1 mM phenylmethylsulfonyl fluoride, 1 mM sodium orthovanadate, 1 mM NaF, 10 μ g/ml aprotinin, 10 μ g/ml leupeptin, and 50 mM Tris-HCl, pH 7.4. The cell lysates were centrifuged at $14,000 \times g$ for 15 min, and the supernatants were separated by SDS-PAGE and transferred to the Optitran nitrocellulose membranes (Schleicher & Schuell, Dassel, Germany). The membranes were blocked and probed with specific antibodies.

Measurement of Cell Surface and Endocytosed $\alpha 1$ Na/K-ATPase—The surface expression of the $\alpha 1$ Na/K-ATPase was measured by biotinylation using the procedures described before (21, 23). In brief, cultured cells were placed on ice and rinsed twice with ice-cold PBS containing 1 mM EDTA for 5 min, which opens tight junctions (23). Then cells were exposed twice to 1.5 mg/ml EZ-Link Sulfo-NHS-SS-Biotin (Pierce) in biotinylation buffer (10 mM triethanolamine, 150 mM NaCl, pH 9.0) for 25 min at 4 °C. Unreacted Sulfo-NHS-SS-Biotin was scavenged by incubation with 100 mM glycine buffer (in PBS) for 20 min. Cells were then solubilized in lysis buffer (1% Triton X-100, 150 mM NaCl, 5 mM EDTA, 50 mM Tris, pH 7.5), and cell lysates were cleared by centrifugation at $14,000 \times g$ for 15 min at 4 °C. Supernatants from different treatment groups (based on equal amounts of protein) were incubated overnight at 4 °C with streptavidin-agarose beads (Pierce). The beads were then washed twice with lysis buffer, twice with high salt buffer (0.1% Triton X-100, 500 mM NaCl, 5 mM EDTA, 50 mM Tris, pH 7.5), and twice with no-salt wash buffer (10 mM Tris, pH 7.5). Bound proteins were eluted with SDS-containing sample buffer and subjected to immunoblot analysis as described above.

Endocytosis of the $\alpha 1$ Na/K-ATPase was measured using a pulse-chase strategy. Biotinylation of cell surface was conducted as described above, and unreacted *N*-hydroxysulfosuccinimidobiotin was quenched with glycine buffer. Then cells were brought back to normal culture conditions for 0 or 30 min at 37 °C, allowing biotinylated surface $\alpha 1$ Na/K-ATPase to be endocytosed. The endocytosis was terminated by washing cells with ice-cold PBS. Afterward, TCEP (Pierce) reducing agent (100 mM TCEP in 50 mM Tris, pH 7.4) was added to cells for 30 min at 4 °C to clear the remaining cell surface-bound biotin. Cell lysates in lysis buffer (1% Triton X-100, 150 mM NaCl, 5 mM EDTA, 50 mM Tris, pH 7.5) were collected. An equal amount of cell lysates (500 μ g of protein) was incubated with streptavidin-agarose beads, and bound proteins were analyzed by Western blotting.

MTT Assay—MTT assay was performed using the MTT cell proliferation assay kit (ATCC). In brief, 6,000 cells/well were cultured overnight and then were exposed to different concentrations of pNaKtide for the indicated time. Ten μ l of MTT reagent was added to each well for 120 min. The formazan crystal was dissolved with detergent, and the *A* value was measured at 570 nm.

Apoptosis Assay—Annexin/PI staining and TUNEL assay were performed using the Vybrant Apoptosis Assay kit (Invit-

rogen) and the TUNEL Apoptosis Detection kit (Upstate), respectively. Briefly, treated cells were resuspended and mixed with Alexa Fluor 488 annexin V/PI in the annexin-binding buffer. Mounted cells were visualized with a Leica DMIRE2 confocal microscope. To detect apoptotic cells in xenografted tumor tissues, the TUNEL assay was performed according to the manufacturer's instructions. Slides containing formalin-fixed, paraffin-embedded tumor sections were deparaffinized and then washed with PBS for 30 min at 37 °C. After incubation with proteinase K (Invitrogen), tumor sections were mixed with terminal deoxynucleotidyltransferase end-labeling mixture (containing Biotin-dUTP, terminal deoxynucleotidyltransferase in terminal deoxynucleotidyltransferase buffer) for 60 min at 37 °C. After blocking, the tumor sections were incubated with avidin-FITC solution for 30 min at 37 °C. Washed tumor sections were further counterstained with PI solution and visualized with a Leica DMIRE2 confocal microscope.

DU145 Xenograft Tumors in NOD/SCID Mice—Animal protocols were approved by the Institutional Animal Care and Use Committee at the University of Toledo Health Science Campus. Tumor xenografts were established by subcutaneous injection of 5×10^6 DU145 cells into the left and right flanks of 6-week-old female NOD/SCID mice (Charles River). Tumor length (L) and width (W) were measured with calipers and tumor volume was estimated as $V = (L \times W^2)/2$. When the tumors reached an average volume of 100 mm³, mice were injected subcutaneously with saline or pNaKtide (at doses of 2 and 10 mg/kg body weight) every other day for five times.

Immunostaining of $\alpha 1$ Na/K-ATPase and Active Src—Cells cultured on coverslips were fixed for 15 min with ice-cold methanol, washed three times with PBS, and then blocked with Signal Enhancer (Invitrogen). The cells were then incubated with a mouse anti-Na/K-ATPase $\alpha 1$ monoclonal antibody (Millipore) or a rabbit anti-phosphotyrosine 418 antibody in PBS containing 1% BSA for 1 h at room temperature. After three washes with PBS, cells were exposed to Alexa Fluor 555-conjugated anti-mouse or Alexa Fluor 488-conjugated anti-rabbit secondary antibody for 1 h at room temperature, washed, and mounted onto slides. Image visualization was performed using a Leica DMIRE2 confocal microscope.

Immunohistochemical (IHC) Staining and Vascularity Analysis—Na/K-ATPase $\alpha 1$ IHC staining was performed by US Biomax (Rockville, MD) using a human prostate tissue microarray (tissue microarray catalog no. PR954; US Biomax), which contains 36 cases of prostate carcinoma and 8 cases of normal tissues. In brief, prostate tissue microarray was deparaffinized, hydrated, and incubated with 3% H₂O₂ to block endogenous peroxidase. Then, tissue sections were subjected to antigen retrieval by using Target Retrieval Solution (Dako Cytomation) and blocked with normal horse blocking serum. Tissue sections were incubated with a mouse monoclonal anti-Na/K-ATPase $\alpha 1$ antibody (Millipore) solution (final concentration 3.3 ng/ μ l) for 1 h at room temperature. Slides were washed and then incubated with ImmPRESS Reagent anti-mouse Ig peroxidase (Vector Laboratories) for 1 h followed by incubation with DAB substrate solution (Dako Cytomation) for 5 min. Slides were mounted, and images were recorded with an Olympus light microscope. Specific IHC staining of Na/K-ATPase $\alpha 1$ yields

brown color at site of the target antigen, whereas hematoxylin counterstaining yields blue color in cell nucleus. Two independent pathologists examined $\alpha 1$ staining intensity and scored each slide three times as defined: 0, absent; 1, weak; 2, moderate; 3, strong. A mean score was recorded.

To assess tumor vascularity in the xenograft tumor tissues, IHC staining of CD31 in tissue sections was performed as described above. A goat polyclonal anti-CD31 antibody (Santa Cruz Biotechnology, sc-1506, final concentration 2 ng/ μ l) and ImmPRESS Reagent anti-goat Ig peroxidase (Vector Laboratories) were used. Negative controls were performed by replacing primary antibody with normal goat immunoglobulins. Then, the CD31-positive regions (in brown) were quantified using ImageJ 1.43, and vascularity density was calculated as the percent of tumor tissue area occupied by vessels as described (24).

Analysis of Data—Data are given as the mean \pm S.E. Differences of formed tumors in response to saline or pNaKtide were calculated with χ^2 test. One-way ANOVA test was used to test the significance in tumor weights and tumor volumes. Statistical significance of data from all other experiments was determined by Student's *t* test. A *p* value of <0.05 was considered significant.

RESULTS

Down-regulation of $\alpha 1$ Na/K-ATPase in Prostate Cancer—As depicted in Fig. 1, A and B, the expression of $\alpha 1$ Na/K-ATPase is significantly reduced in human prostate carcinoma as measured by IHC staining. Although most of the control samples exhibited moderate to strong staining, >50% of prostate carcinoma samples (20 samples of a total of 36) had a weak staining. Moreover, about 11% of samples (4 of a total of 36) were actually scored absent for $\alpha 1$ Na/K-ATPase. To verify these findings and to establish an *in vitro* model for further investigation, we conducted the following studies in three human prostate cancer cell lines that exhibit different metastatic potentials (25). Normal human prostate epithelial RWPE-1 cells and LLC-PK1 cells, a noncancerous renal epithelial cell line used extensively in our prior studies of Na/K-ATPase-mediated signal transduction (7, 22), were used as controls. As shown in Fig. 1C, significant reduction in the total cellular $\alpha 1$ Na/K-ATPase was noted in DU145 and PC-3 cell lysates. Because the $\alpha 1$ Na/K-ATPase regulates mainly the plasma membrane, not cytoplasmic, pool of Src, we immunostained these cells with anti- $\alpha 1$ antibody and examined the cellular distribution of $\alpha 1$ Na/K-ATPase. As depicted in Fig. 2A, the $\alpha 1$ subunit resided mainly in the plasma membrane in control cell lines. This pool of $\alpha 1$ Na/K-ATPase is significantly reduced in cancer cell lines. Quantitative analyses using line scanning reveal a reduction of about 15, 50, and 75% in the plasma membrane area across the LNCaP, DU145, and PC-3 cells, respectively (Fig. 2B). These reductions were further confirmed by surface biotinylation assays (Fig. 2D). Interestingly, a high level of diffused and vesicular $\alpha 1$ staining relative to the plasma membrane signal was noted in DU145 and PC-3 cells (Fig. 2C) after increasing the laser intensity. These findings suggest an increased endocytosis of $\alpha 1$ Na/K-ATPase in these cells. To test this further, a pulse-chase experiment was performed to measure the endocytosed $\alpha 1$ in DU145 cells directly. Surface-biotinylated cells were brought back to normal culture

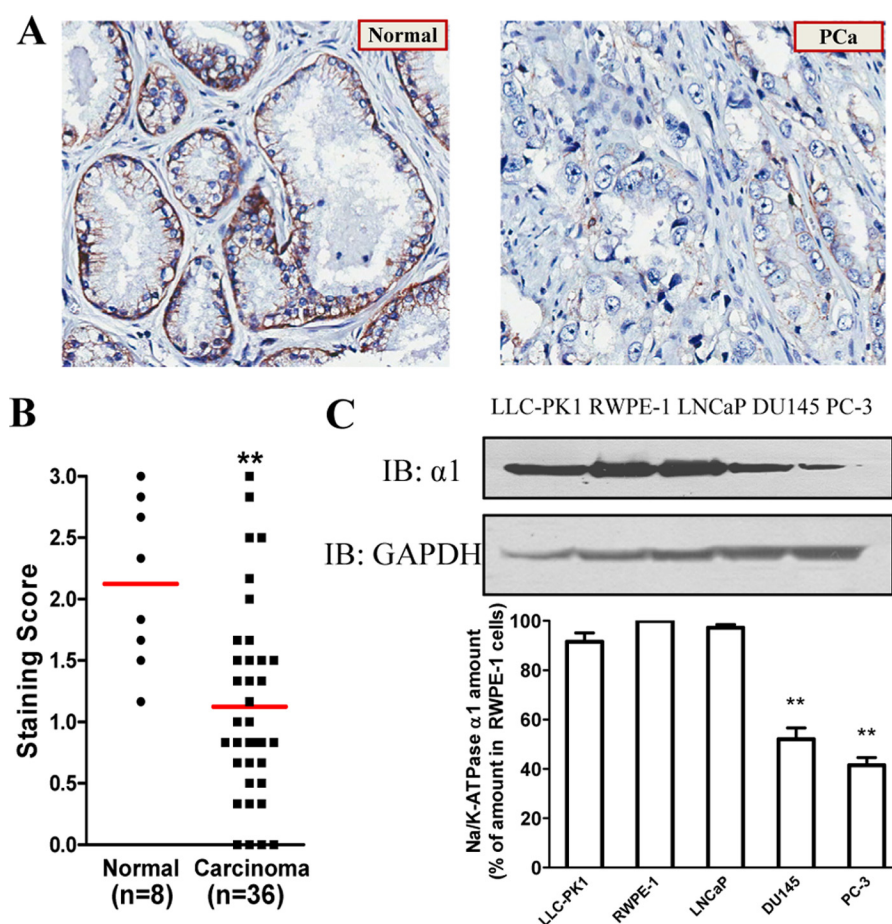


FIGURE 1. Down-regulation of $\alpha 1$ Na/K-ATPase in prostate cancer cells. A, $\alpha 1$ expression patterns in paired human normal prostate tissue (left) and carcinoma (right). Human tissue arrays were immunostained with monoclonal antibody against $\alpha 1$ (in brown). Hematoxylin was used for counterstaining of cell nucleus (in blue). B, $\alpha 1$ staining score in prostate tissues. Staining intensity was scored as absent (0), weak (1), moderate (2), or strong (3). Two independent pathologists scored each slide three times. C, expression of Na/K-ATPase $\alpha 1$ subunit in cultured cells. Equal amounts of whole cellular proteins (20 μ g) from confluent cells were subjected to Western blot analysis with the anti- $\alpha 1$ antibody. The upper panel shows representative blots of $\alpha 1$ and GAPDH, and the lower panel shows the quantification data of $\alpha 1$ intensity from four independent experiments. *, $p < 0.05$; **, $p < 0.01$. Error bars, S.D.

condition for different times, and then surface-bound biotin was cleared using TCEP. The remaining biotinylated intracellular pool of $\alpha 1$ was analyzed. Because a large number of RWPE-1 cells detached from culture dish during TCEP treatment, LLC-PK1 cells were used as a control. As shown in Fig. 2E, there was no endocytosed $\alpha 1$ detected at 0 min, suggesting that TCEP cleavage was complete. After recovery for 30 min, much more (about three times) $\alpha 1$ was endocytosed in DU145 than that in LLC-PK1 cells. Considering the difference in the membrane $\alpha 1$ amount in these two cell lines (Fig. 2, B and D), the $\alpha 1$ endocytosis/30 min in DU145 cells could be 9–10 times of that in LLC-PK1 cells.

As depicted in Fig. 3A, the amount of active Src or Src family kinases was significantly elevated in human cancer cells. Because reduction of the $\alpha 1$ preferentially affects the Src-interacting pool of Na/K-ATPase (11, 21), this increase in Src activity could be due to the down-regulation of $\alpha 1$ Na/K-ATPase in these cells. If this is a case, it is likely that addition of $\alpha 1$ mimetic peptide would be able to inhibit Src and then cancer cell growth. To test this possibility, we transfected DU145 cells with YFP-ND1 and evaluated its effect on cell growth. The ND1 peptide is derived from the N domain of $\alpha 1$ subunit (residues 379–435) and binds and inhibits Src (10). As depicted in sup-

plemental Fig. S1A, the expression of YFP-ND1 was detected as early as 6 h after transfection and peaked at 24 h in DU145 cells. Notably, a significant decrease in the percentage of cells with YFP fluorescence was observed after 36 h in the YFP-ND1-transfected, but not YFP-transfected, cells. Moreover, a large number of YFP-ND1-expressing cells rounded up and detached from the dish (supplemental Fig. S1A). When trypan blue-negative cells were counted, expression of YFP-ND1 caused a >40% decrease in the number of cells (supplemental Fig. S1B). Taken together, these findings indicate that the expression of ND1 has drastic effects on cell viability.

pNaKtide Attenuates Activities of Src and Src Effectors—In view of the above findings, we next tested whether the ND1-derived pNaKtide can inhibit activities of Src and Src effectors in human cancer cells. As shown in Fig. 3A, pNaKtide had no effect on basal Src activity in LLC-PK1 cells as we reported previously (10). However, it caused a significant inhibition of the membrane pool of Src in all three cancer cell lines. To confirm this finding, cell lysates from control and pNaKtide-treated DU145 cells were subjected to Western blotting. As depicted in Fig. 3B, pNaKtide inhibited Src in DU145 cells. Moreover, pNaKtide inhibited known Src effectors such as FAK and ERKs in DU145 cells (Fig. 3B). Finally, pNaKtide

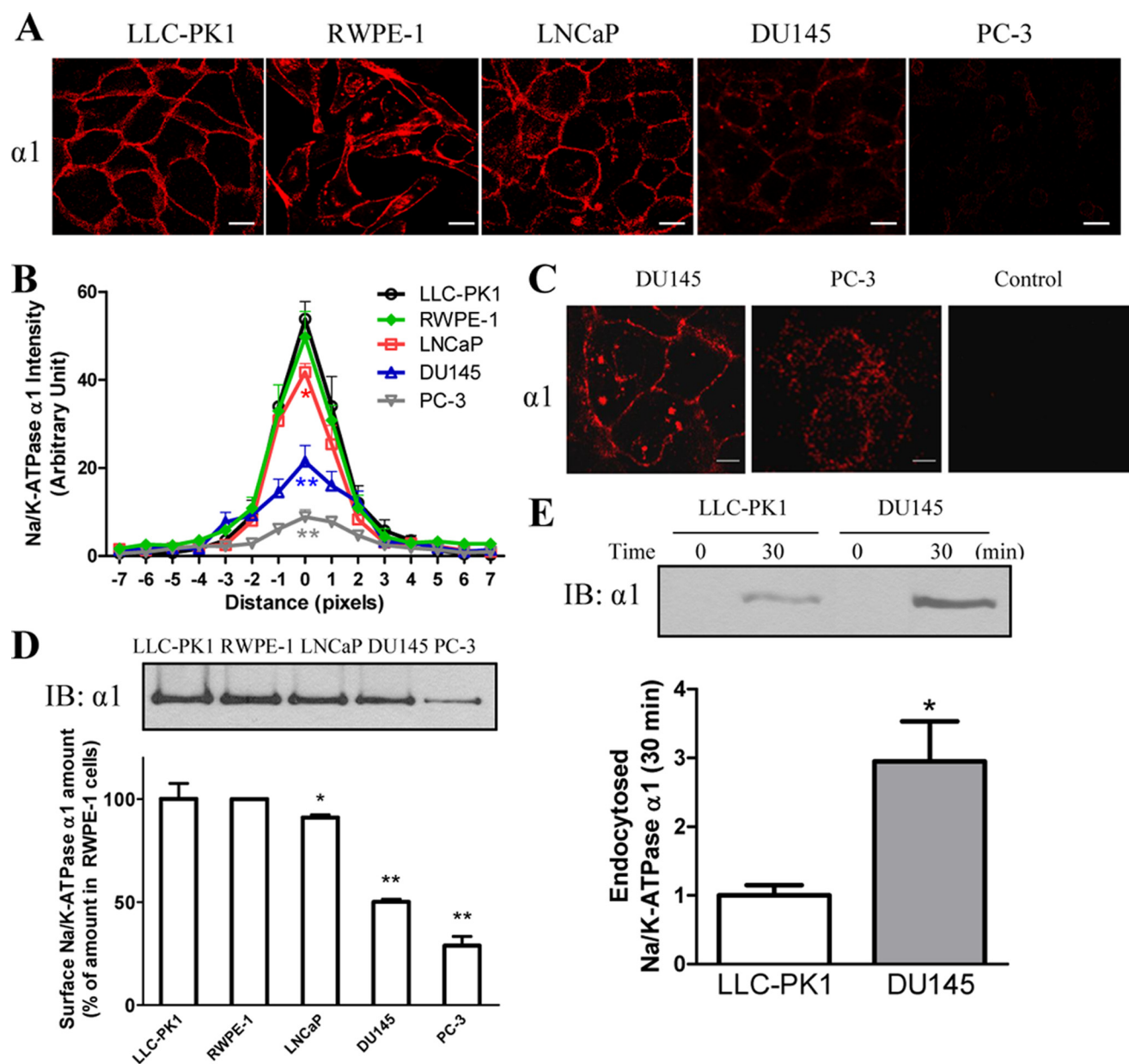


FIGURE 2. Decreases in surface expression of $\alpha 1$ Na/K-ATPase in prostate cancer cells. A, cellular distribution of $\alpha 1$ Na/K-ATPase. The fixed cells were immunostained with anti- $\alpha 1$ antibody and visualized (in red) with a Leica DMIRE2 confocal microscope. Representative images from four independent experiments are shown. Scale bars, 5 μ m. B, line scan quantitation of $\alpha 1$ staining intensity across the cell membrane. The $\alpha 1$ intensity was line scan-quantified using ImageJ. The x axis is defined as distance (in pixel units) from cell membrane where the highest $\alpha 1$ staining intensity is. The y axis is the arbitrary units of quantified staining intensity within each pixel unit. Thirty individual cells from three separate experiments were used to collect these data. C, cellular distribution of $\alpha 1$ in DU145 and PC-3 cells after higher intensity laser was applied. Scale bars, 8 μ m. D, cell surface $\alpha 1$ in cultured cells. Biotinylated cell surface proteins were analyzed for $\alpha 1$ by Western blotting. Representative blots from three independent experiments are shown. Error bars, S.D. E, endocytosed $\alpha 1$ in cultured cells. The upper panel depicts a typical immunoblot of biotinylated $\alpha 1$ Na/K-ATPase after 0- and 30-min recovery. The assays were conducted as described under "Experimental Procedures." Quantified data from three independent experiments are shown in the lower panel relative to LLC-PK1. *, $p < 0.05$; **, $p < 0.01$.

was also capable of reducing the expression of c-Myc (Fig. 3B) that is known to play an important role in prostate cancer development. These data together indicate that pNaKtide could be used to attenuate the elevated activities of Src, Src effectors, and c-Myc in cancer cells. It is important to note that pNaKtide is apparently specific to the $\alpha 1$ -interacting pool of Src because although pNaKtide had no effect on basal Src activity in LLC-PK1 cells (Fig. 2A and Ref. 10), it did produce a significant inhibition of Src in LLC-PK1-derived TCN23-19 cells (supplemental Fig. S2) where the Na/K-

ATPase-interacting pool of Src is freed by 90% knockdown of the $\alpha 1$ subunit (11).

Effects of pNaKtide on Cell Growth—Src is known to play an important role in regulating cell growth and apoptosis (12). We therefore evaluated the growth-inhibitory effects of pNaKtide using MTT analysis. A time-dependent growth inhibition in DU145 cells is presented in Fig. 4A. It is important to note that pNaKtide also affected cell viability, which is apparent at higher concentrations (e.g. 1 and 5 μ M). When dose-dependent effects were measured in all three cancer cell lines, we found that

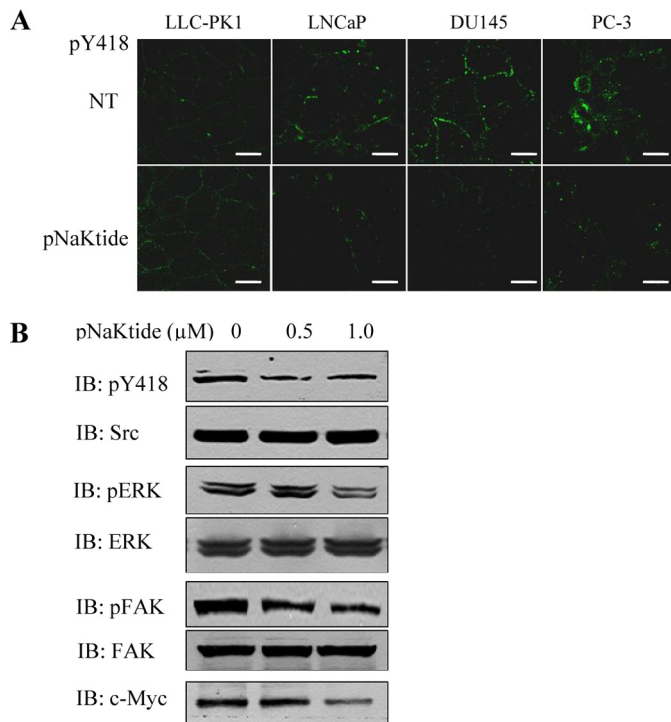


FIGURE 3. Effects of $\alpha 1$ mimetics on Src signaling in DU145 cells. *A*, active Src in control or pNaKtide-treated ($1 \mu\text{M}$ for 1 h) cells. Cells on coverslips were fixed with ice-cold methanol, then immunostained using anti-phosphotyrosine 418 antibody. Fluorescence of Src phosphotyrosine 418 was visualized (in green) with a Leica DMIRE2 confocal microscope. Representative images from three separate experiments are shown. Scale bars, $5 \mu\text{m}$. *B*, regulation of Src and Src effectors by pNaKtide. DU145 cells were exposed to pNaKtide at the indicated concentrations for 1 h. Cell lysates were analyzed for Src, ERK, and FAK phosphorylation as well as c-Myc by Western blotting. Representative blots from three independent experiments are shown.

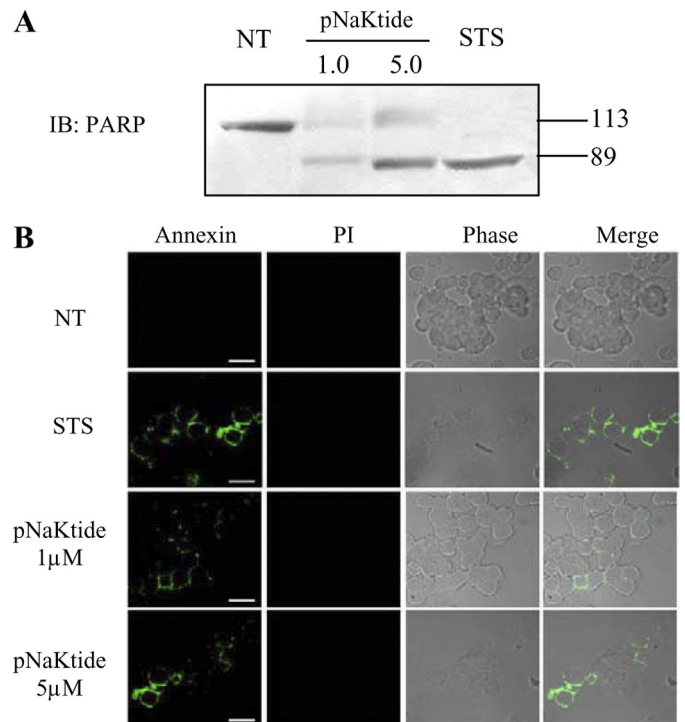


FIGURE 5. Induction of apoptosis by pNaKtide in DU145 cells. *A*, PARP cleavage induced by pNaKtide. The DU145 cells were exposed to pNaKtide or $0.5 \mu\text{M}$ staurosporine (STS) for 24 h. The attached and detached cells from the culture media were collected and analyzed for PARP by Western blotting. Representative blots from three independent experiments are shown. NT, not treated. *B*, annexin V/PI staining of DU145 cells in the absence or presence of pNaKtide. Upon treatment, DU145 cells were stained with annexin V and counterstained with PI using the Vybrant apoptosis kit. Annexin V (in green) and PI (in red) were visualized using a Leica DMIRE2 confocal microscope. Representative images of four independent studies are shown. Scale bar, $12 \mu\text{m}$.

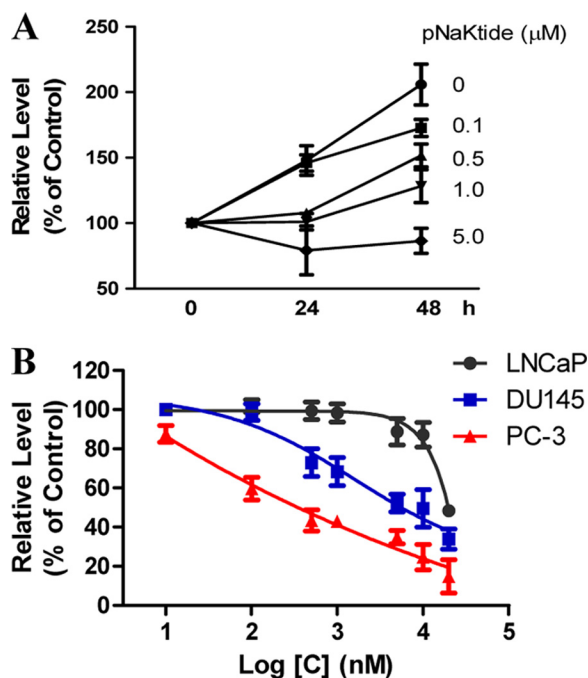


FIGURE 4. Effect of pNaKtide on DU145 cell proliferation. Cells were seeded in 96-well plates and exposed to pNaKtide as the function of times (*A*) or doses (*B*). MTT assay was performed according to the instructions from ATCC. $n = 4$. Error bars, S.D.

LNCaP cells were most resistant to pNaKtide, whereas PC-3 cells were highly sensitive (Fig. 4*B*). The EC_{50} value of pNaKtide was 100 nM , $5 \mu\text{M}$, and $20 \mu\text{M}$ in PC-3, DU145, and LNCaP cells, respectively. As a control, we repeated this set of experiments with pC1 (10). Like pNaKtide, pC1 is tagged with TAT leader sequence, and it is also distributed in the cell membrane (data not shown). We found that pC1 did not have any inhibitory effect in the MTT assay up to $20 \mu\text{M}$.

Because pNaKtide affects cell viability, we tested whether pNaKtide stimulates apoptosis in DU145 cells using the following two sets of experiments. Staurosporine was used as a positive control. First, we measured the effect of pNaKtide on the cleavage of PARP (26, 27). As shown in Fig. 5*A*, like staurosporine, pNaKtide (1 and $5 \mu\text{M}$) stimulated PARP cleavage in DU145 cells. To verify the apoptotic effect of pNaKtide, annexin V/PI staining was performed. Like staurosporine, pNaKtide produced a clear membrane staining of annexin V without nuclear PI staining (Fig. 5*B*).

pNaKtide Inhibits DU145 Xenograft Growth—Because the above *in vitro* studies indicate that pNaKtide can inhibit Src/FAK/ERK and c-Myc pathways in human prostate cancer cells, we tested whether it would inhibit the tumor xenograft growth *in vivo*. DU145 cells were chosen for the test because their sensitivity to pNaKtide is between PC-3 and LNCaP cells. In the first set of studies, cells were treated with $1 \mu\text{M}$ pC1 or pNaKtide

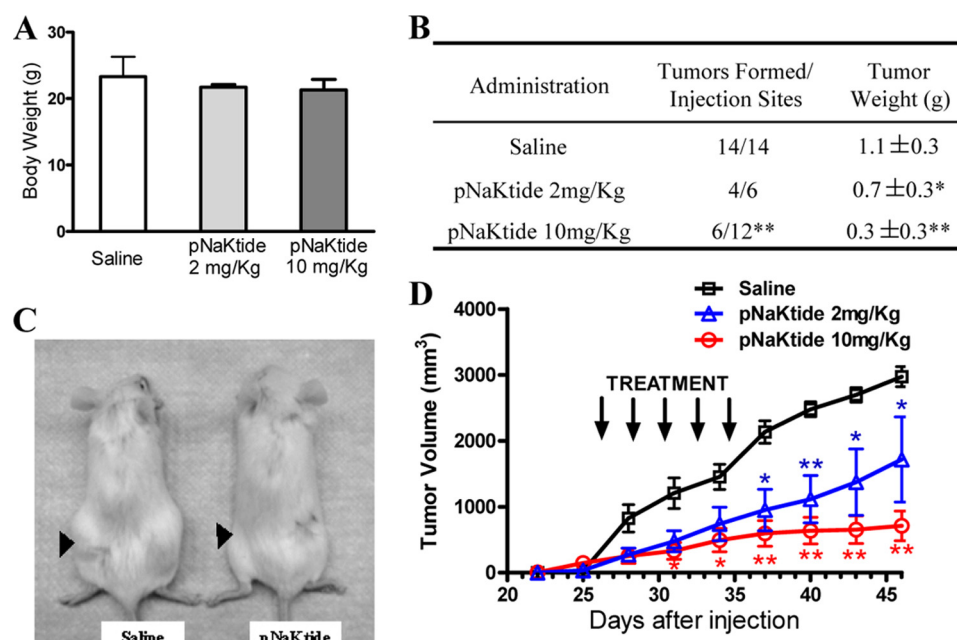


FIGURE 6. Effect of pNaKtide on the growth of DU145 xenografts in NOD/SCID mice. DU145 cells (5×10^6) were injected subcutaneously in the flank of NOD/SCID mice. After mean tumor volume reached 100 mm^3 , and mice were injected with saline or pNaKtide at a dose of 2 or 10 mg/kg. **A**, average body weight of the NOD/SCID mice after administration of pNaKtide. Error bars, S.D. **B**, tumor formation in NOD/SCID mice. The average tumor weight values were from four and six tumors of 2 mg/kg and 10 mg/kg pNaKtide-treated groups, respectively. **C**, mice bearing xenograft tumors. Arrowheads identify the location of the tumors. **D**, growth of DU145 xenograft tumors in NOD/SCID mice treated with saline or pNaKtide. *, $p < 0.05$; **, $p < 0.01$.

for 60 min and washed. Afterward, 5×10^6 control peptide or pNaKtide-treated trypan blue-negative DU145 cells were injected subcutaneously into 4–6-week-old NOD/SCID mice. We found that this treatment resulted in a significant reduction in tumor weight *in vivo* (tumor weight: pC1, $1.2 \pm 0.2 \text{ g}$, $n = 6$, versus pNaKtide, $0.6 \pm 0.2 \text{ g}$, $n = 6$; $p < 0.01$) after 45 days. However, this regimen of treatment is much less effective in inhibiting tumor growth than that of repeated dosing (see next paragraph).

To test whether pNaKtide can reduce the growth or cause regression of an existing tumor, we used three groups of 4–6-week-old NOD/SCID mice and injected them subcutaneously with 5×10^6 DU145 cells. The treatment with pNaKtide (in saline) or vehicle was initiated after the tumors reached an average volume of 100 mm^3 . As depicted in Fig. 6, A–C, pNaKtide treatment produced a dose-dependent inhibition of tumor growth. When 10 mg/kg pNaKtide was administered once every 2 days for five times, it resulted in $>75\%$ inhibition in both tumor volume (Fig. 6D) and weight (Fig. 6B) even after stopping administration of pNaKtide for >10 days. Moreover, half of tumors regressed after pNaKtide treatment and were not detected in final necropsy (Fig. 6B). Interestingly, although two of seven mice in the control group showed severe metastasis, none was detected in pNaKtide-treated groups.

To test whether pNaKtide treatment affects Src expression and Src activity, we measured total Src and Src Tyr-418 phosphorylation in the xenograft tumor homogenates. Consistent with the observation in cultured cells (Fig. 3), significant inhibition of Src was found in pNaKtide-treated tumor homogenates (Fig. 7A). However, pNaKtide treatment had no effect on the amount of total Src.

Finally, we performed hematoxylin & eosin (H&E) staining of DU145 xenograft tumors. As depicted in Fig. 7B, untreated

tumors showed compact cell distribution patterns with dark

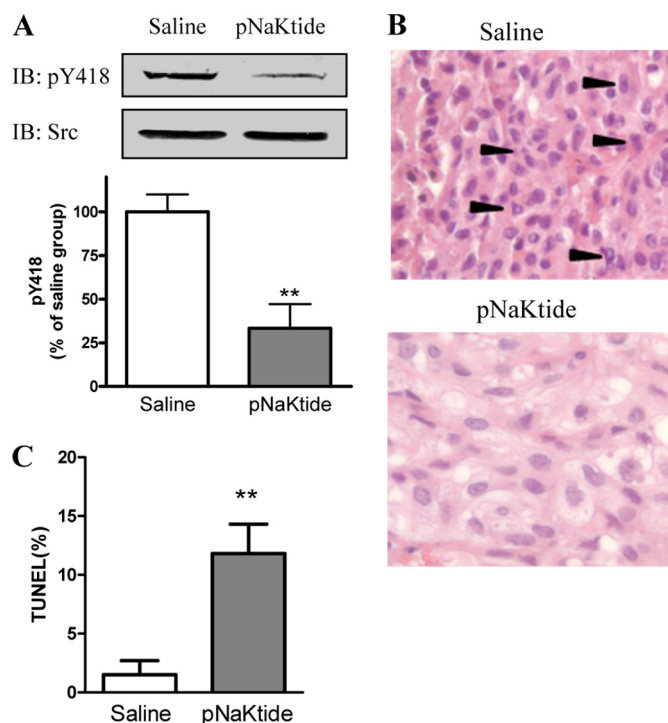


FIGURE 7. Characterization of xenograft tumors. Fourteen tumors in the saline group and six tumors in the 10 mg/kg pNaKtide group were analyzed. **A**, effects of pNaKtide on Src. Tumor homogenates from saline and pNaKtide groups were analyzed for total Src and Src phosphotyrosine 418 by Western blotting. Quantitative data were collected as the phosphotyrosine 418/Src ratio from tumor samples. Error bars, S.D. **B**, H&E staining of the formalin-fixed, paraffin-embedded xenograft tumors. Original magnifications, $\times 600$. Arrowheads indicate cells in mitosis. **C**, TUNEL assay of xenograft tumors. TUNEL assay was performed using the TUNEL Apoptosis Detection kit, and percent of TUNEL-positive cells was quantified. **, $p < 0.01$.

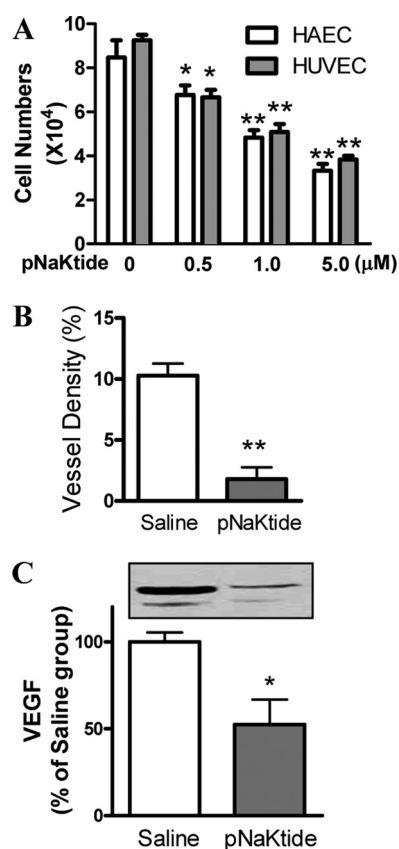


FIGURE 8. Effects of pNaKtide on angiogenesis. A, inhibition of endothelial cell proliferation by pNaKtide. Human umbilical vein endothelial cells (HUVECs)/human aortic endothelial cells (HAECs) cultured in 12-well plates were exposed to pNaKtide at the indicated concentrations for 72 h. Then, trypan blue-negative cells were counted. Data from four independent experiments were collected. Error bars, S.D. B, vessel density of xenograft tumors. IHC staining of CD31 in the formalin-fixed, paraffin-embedded xenograft tumors (14 in saline group and 6 in 10 mg/kg pNaKtide group) was performed to identify the vessels. Then, the vessel density was calculated as the percent of tumor area occupied by vessels. C, expression of VEGF in tumor homogenates. VEGF levels in the saline or pNaKtide-treated tumors were evaluated by Western blotting using anti-VEGF antibody. *, $p < 0.05$; **, $p < 0.01$.

blue nuclear staining in the vehicle group, suggesting that these tumor cells were highly proliferative. Accordingly, there were some cells with prominent nucleoli under stages of mitosis (arrowheads in Fig. 7B). Treatment with pNaKtide resulted in a decrease in cell population and cell division. In addition, more TUNEL-positive cells were found in pNaKtide-treated tumors than in control groups (Fig. 7C).

Inhibition of Tumor Angiogenesis by pNaKtide—Tumor growth and metastasis are highly dependent on angiogenesis (28). Interestingly, when tumors were collected from both control and pNaKtide-treated mice, we noticed that tumors in the pNaKtide-treated group were much paler than those from the control mice, suggesting that pNaKtide treatment might inhibit angiogenesis. To verify, we first assessed the effect of pNaKtide on the proliferation of cultured human endothelial cells because endothelial cell proliferation is the prerequisite of angiogenesis. As shown in Fig. 8A, pNaKtide inhibited the proliferation of both human umbilical vein endothelial cells and human aortic endothelial cells in a dose-dependent manner. To test further the ability of pNaKtide to inhibit *in vivo* angiogenesis, tumors from control and pNaKtide-treated animals were

immunostained with an antibody against CD31 to identify vessels. The vessel density of tumors from control mice was approximately 10%, and pNaKtide treatment reduced the density to approximately 2.5% (Fig. 8B). Moreover, when the production of VEGF, an angiogenic factor, was measured in tumor homogenates, we found that pNaKtide treatment produced a >50% reduction in total VEGF (Fig. 8C). Taken together, these findings indicate that pNaKtide inhibits tumor angiogenesis.

DISCUSSION

In this report, we show that the plasma membrane pool of $\alpha 1$ Na/K-ATPase is significantly reduced in prostate cancer cells. We further demonstrate that supplement of the $\alpha 1$ mimetic peptide (e.g. ND1 or pNaKtide) decreases activities of Src and Src effectors and consequently inhibits cancer cell growth. Furthermore, administration of pNaKtide potentially inhibits the angiogenesis, stimulates apoptosis, and reduces the xenografted tumor size in the NOD/SCID mice. These conclusions and other important issues are discussed further.

Potential Role of Na/K-ATPase in Regulation of Tumor Growth—A decrease in $\alpha 1$ Na/K-ATPase expression has been noted in several human cancers, including pancreatic (29), colorectal (30), bladder (31), and kidney (32). Moreover, prior studies have also documented the down-regulation of $\beta 1$ subunit of Na/K-ATPase in several kidney cancer cell lines (33). We report here a significant reduction in $\alpha 1$ Na/K-ATPase in human prostate carcinoma as well as in highly metastatic prostate cancer cell lines including DU145 and PC-3. The most significant reduction in $\alpha 1$ (>50%) was detected in the plasma membrane of these cells (Fig. 2, A, B, and D). Moreover, we observed an increased endocytosis of $\alpha 1$ Na/K-ATPase in DU145 cells (Fig. 2E). Thus, post-translational regulation may play an important role in the down-regulation of $\alpha 1$ Na/K-ATPase in these cells.

Because prostate cancer cells, in general, do not need as much Na/K-ATPase to pump as do the normal epithelial cells, the observed down-regulation of $\alpha 1$ Na/K-ATPase might be expected. However, recent studies have revealed that the $\alpha 1$ Na/K-ATPase has many nonpumping functions that could play an important role in regulation of cell migration and growth. For example, the formation of tight junction in epithelia requires the expression of Na/K-ATPase (34). Moreover, the β subunit is known to play an important role in cell/cell adhesion as well as cell/matrix interaction (35). Interestingly, repletion of $\beta 1$ subunit appears to be sufficient to reduce the migration and tumor formation of kidney cancer cells (36). Furthermore, we have recently demonstrated an important role of Na/K-ATPase $\alpha 1$ subunit in regulation of cellular kinase activity through its interaction with c-Src in the plasma membrane (7, 8, 11, 37). Therefore, we suggest that the reduction in the plasma membrane $\alpha 1$ could affect the growth of tumor in several ways. First, the down-regulation of $\alpha 1$ Na/K-ATPase might make it less effective for Na/K-ATPase to interact with and then inhibit cellular Src. This would increase basal Src and FAK activity and consequently promote epithelial cell proliferation, migration, and invasion (34, 38, 39). Consistently, we found that metastatic prostate cancer cells are highly sensitive to the addition of the Na/K-ATPase $\alpha 1$ mimetics, including ND1 (supplemental Fig. S1)

and pNaKtide (Fig. 4). Second, a decrease in the plasma membrane Na/K-ATPase $\alpha 1$ would impair the ability of cells to provide a counterregulation of Src and other growth-promoting pathways, especially in cellular structures such as tight junctions and adhesions where the Na/K-ATPase is highly concentrated in normal epithelial cells. This could occur when cellular Src is activated by steroid hormone/receptor interaction (40, 41) or other factors such as increased activity of human epidermal growth factor receptor (42). Finally, increases in Src activity due to the down-regulation of $\alpha 1$ could potentiate VEGF production and then promote angiogenesis. Needless to say, the potential role of Na/K-ATPase in control of tumor growth needs to be tested further in animal models.

Na/K-ATPase as a Target for Developing Novel Anticancer Therapeutics—To our knowledge, this is the first report to show that $\alpha 1$ Na/K-ATPase mimetic peptides are effective in inducing apoptosis in prostate cancer cells (Fig. 5). Moreover, two different sets of experiments demonstrate that pNaKtide is highly effective in blocking the growth of DU145 xenograft *in vivo*. First, we found that pretreatment of DU145 cells with pNaKtide caused a significant reduction in tumor size. Although it is unlikely that the activity of pNaKtide loaded into DU145 cells during a 1-h exposure would last for 45 days *in vivo*, its effects on cell growth during the first few days could produce this reduction in tumor size. This mode of action has been demonstrated with other compounds (43). Second, we found that repeated dosing (once every 2 days for a total of five times) was more effective in reducing tumor size than that of 1-h exposure. Moreover, repeated dosing appears to be capable of inducing tumor regression and preventing tumor metastasis. Of course, these effects need to be further verified.

Mechanistically, pNaKtide stimulates apoptosis, inhibits cell growth, and decreases tumor angiogenesis (Figs. 4 and 8). Some of these effects are likely related to the Src inhibitory action of pNaKtide. However, pNaKtide is unique in the way it regulates cellular Src. First, pNaKtide is not an ATP mimetic and thus works differently from this class of small molecular Src inhibitors (44–47). Second, it is derived from a widely expressed endogenous protein (10). Third, a majority of pNaKtide appears to be localized in the plasma membrane (10) where the active Src resides. This action mechanism explains why only marginal cellular Src activity is inhibited by pNaKtide (Fig. 3) in normal epithelial cells, whereas small molecule ATP mimetic produced a complete inhibition (44). This is also consistent with the finding that pNaKtide is less effective in inhibiting the growth of LNCaP cells where a large pool of $\alpha 1$ Na/K-ATPase is expressed in the plasma membrane. On the other hand, pNaKtide becomes highly effective for more metastatic cells such as DU145 and PC-3 where the plasma membrane pool of Na/K-ATPase is significantly reduced (Fig. 2). Thus, the effect of pNaKtide appears to be highly selective.

Because peptides are normally vulnerable to peptidase degradation, more studies are needed to characterize further the stability of pNaKtide *in vivo*. Absorption and metabolism of pNaKtide in whole animals remain to be assessed. It would also be important to characterize the distribution and stability of pNaKtide in tumor samples. Nevertheless, our studies here clearly demonstrate the anticancer efficacy of pNaKtide *in vivo*.

Finally, it has not escaped our notice that increased expression of the Na/K-ATPase $\alpha 1$ could present another strategy to target the $\alpha 1$ Na/K-ATPase-mediated signal transduction in cancer cells. However, effective compounds remain to be discovered and tested.

Acknowledgments—We thank Dr. Guiyuan Li at University of Toledo for assistance with pathological studies and Martha Heck for editing the manuscript.

REFERENCES

- Kaplan, J. H. (2002) *Annu. Rev. Biochem.* **71**, 511–535
- Skou, J. C. (1957) *Biochim. Biophys. Acta* **23**, 394–401
- Cai, T., Wang, H., Chen, Y., Liu, L., Gunning, W. T., Quintas, L. E., and Xie, Z. J. (2008) *J. Cell Biol.* **182**, 1153–1169
- Rajasekaran, A. K., and Rajasekaran, S. A. (2003) *Am. J. Physiol. Renal Physiol.* **285**, F388–396
- Li, Z., and Xie, Z. (2009) *Pflugers Arch.* **457**, 635–644
- Tian, J., and Xie, Z. J. (2008) *Physiology* **23**, 205–211
- Tian, J., Cai, T., Yuan, Z., Wang, H., Liu, L., Haas, M., Maksimova, E., Huang, X. Y., and Xie, Z. J. (2006) *Mol. Biol. Cell* **17**, 317–326
- Chen, Y., Cai, T., Wang, H., Li, Z., Loreaux, E., Lingrel, J. B., and Xie, Z. (2009) *J. Biol. Chem.* **284**, 14881–14890
- Ye, Q., Li, Z., Tian, J., Xie, J. X., Liu, L., and Xie, Z. (2011) *J. Biol. Chem.* **286**, 6225–6232
- Li, Z., Cai, T., Tian, J., Xie, J. X., Zhao, X., Liu, L., Shapiro, J. I., and Xie, Z. (2009) *J. Biol. Chem.* **284**, 21066–21076
- Liang, M., Cai, T., Tian, J., Qu, W., and Xie, Z. J. (2006) *J. Biol. Chem.* **281**, 19709–19719
- Thomas, S. M., and Brugge, J. S. (1997) *Annu. Rev. Cell Dev. Biol.* **13**, 513–609
- Yeatman, T. J. (2004) *Nat. Rev. Cancer* **4**, 470–480
- Irby, R. B., and Yeatman, T. J. (2000) *Oncogene* **19**, 5636–5642
- Ma, Y. C., Huang, J., Ali, S., Lowry, W., and Huang, X. Y. (2000) *Cell* **102**, 635–646
- Migliaccio, A., Castoria, G., Di Domenico, M., de Falco, A., Bilancio, A., Lombardi, M., Barone, M. V., Ametrano, D., Zannini, M. S., Abbondanza, C., and Auricchio, F. (2000) *EMBO J.* **19**, 5406–5417
- Kaplan, K. B., Swedlow, J. R., Varmus, H. E., and Morgan, D. O. (1992) *J. Cell Biol.* **118**, 321–333
- Kaplan, K. B., Bibbins, K. B., Swedlow, J. R., Arnaud, M., Morgan, D. O., and Varmus, H. E. (1994) *EMBO J.* **13**, 4745–4756
- Wang, Y., Botvinick, E. L., Zhao, Y., Berns, M. W., Usami, S., Tsien, R. Y., and Chien, S. (2005) *Nature* **434**, 1040–1045
- Sandilands, E., Brunton, V. G., and Frame, M. C. (2007) *J. Cell Sci.* **120**, 2555–2564
- Liang, M., Tian, J., Liu, L., Pierre, S., Liu, J., Shapiro, J., and Xie, Z. J. (2007) *J. Biol. Chem.* **282**, 10585–10593
- Haas, M., Wang, H., Tian, J., and Xie, Z. (2002) *J. Biol. Chem.* **277**, 18694–18702
- Gottardi, C. J., Dunbar, L. A., and Caplan, M. J. (1995) *Am. J. Physiol. Renal Physiol.* **268**, F285–295
- Wang, G. M., Kovalenko, B., Wilson, E. L., and Moscatelli, D. (2007) *Prostate* **67**, 968–975
- Aalinkkeel, R., Nair, M. P., Sufrin, G., Mahajan, S. D., Chadha, K. C., Chawda, R. P., and Schwartz, S. A. (2004) *Cancer Res.* **64**, 5311–5321
- Nicholson, D. W., Ali, A., Thornberry, N. A., Vaillancourt, J. P., Ding, C. K., Gallant, M., Gareau, Y., Griffin, P. R., Labelle, M., Lazebnik, Y. A., et al. (1995) *Nature* **376**, 37–43
- Lazebnik, Y. A., Kaufmann, S. H., Desnoyers, S., Poirier, G. G., and Earnshaw, W. C. (1994) *Nature* **371**, 346–347
- Folkman, J. (2006) *Annu. Rev. Med.* **57**, 1–18
- Yamanaka, Y., Onda, M., Uchida, E., Yokomuro, S., Hayashi, T., Kobayashi, T., Sasajima, K., Shirota, T., Tajiri, T., Egami, K., et al. (1989) *Nippon Ika Daigaku Zasshi* **56**, 579–583

30. Sakai, H., Suzuki, T., Maeda, M., Takahashi, Y., Horikawa, N., Minamimura, T., Tsukada, K., and Takeguchi, N. (2004) *FEBS Lett.* **563**, 151–154
31. Espineda, C., Seligson, D. B., James Ball, W., Jr., Rao, J., Palotie, A., Horvath, S., Huang, Y., Shi, T., and Rajasekaran, A. K. (2003) *Cancer* **97**, 1859–1868
32. Seligson, D. B., Rajasekaran, S. A., Yu, H., Liu, X., Eeva, M., Tze, S., Ball, W., Jr., Horvath, S., deKernion, J. B., and Rajasekaran, A. K. (2008) *J. Urol.* **179**, 338–345
33. Rajasekaran, S. A., Ball, W. J., Jr., Bander, N. H., Liu, H., Pardee, J. D., and Rajasekaran, A. K. (1999) *J. Urol.* **162**, 574–580
34. Rajasekaran, S. A., Hu, J., Gopal, J., Gallemore, R., Ryazantsev, S., Bok, D., and Rajasekaran, A. K. (2003) *Am. J. Physiol. Cell Physiol.* **284**, C1497–1507
35. Barwe, S. P., Anilkumar, G., Moon, S. Y., Zheng, Y., Whitelegge, J. P., Rajasekaran, S. A., and Rajasekaran, A. K. (2005) *Mol. Biol. Cell* **16**, 1082–1094
36. Inge, L. J., Rajasekaran, S. A., Yoshimoto, K., Mischel, P. S., McBride, W., Landaw, E., and Rajasekaran, A. K. (2008) *Histol. Histopathol.* **23**, 459–467
37. Ferrandi, M., Molinari, I., Barassi, P., Minotti, E., Bianchi, G., and Ferrari, P. (2004) *J. Biol. Chem.* **279**, 33306–33314
38. Rajasekaran, S. A., Barwe, S. P., Gopal, J., Ryazantsev, S., Schneeberger, E. E., and Rajasekaran, A. K. (2007) *Am. J. Physiol. Gastrointest. Liver Physiol.* **292**, G124–133
39. Contreras, R. G., Shoshani, L., Flores-Maldonado, C., Lázaro, A., and Cerejido, M. (1999) *J. Cell Sci.* **112**, 4223–4232
40. Desai, S. J., Ma, A. H., Tepper, C. G., Chen, H. W., and Kung, H. J. (2006) *Cancer Res.* **66**, 10449–10459
41. Guo, Z., Dai, B., Jiang, T., Xu, K., Xie, Y., Kim, O., Nesheiwat, I., Kong, X., Melamed, J., Handratta, V. D., Njar, V. C., Brodie, A. M., Yu, L. R., Veenstra, T. D., Chen, H., and Qiu, Y. (2006) *Cancer Cell* **10**, 309–319
42. Ishizawar, R., and Parsons, S. J. (2004) *Cancer Cell* **6**, 209–214
43. Gilbert, C. A., Daou, M. C., Moser, R. P., and Ross, A. H. (2010) *Cancer Res.* **70**, 6870–6879
44. Chang, Y. M., Bai, L., Liu, S., Yang, J. C., Kung, H. J., and Evans, C. P. (2008) *Oncogene* **27**, 6365–6375
45. Lara, P. N., Jr., Longmate, J., Evans, C. P., Quinn, D. I., Twardowski, P., Chatta, G., Posadas, E., Stadler, W., and Gandara, D. R. (2009) *Anticancer Drugs* **20**, 179–184
46. Tatarov, O., Mitchell, T. J., Seywright, M., Leung, H. Y., Brunton, V. G., and Edwards, J. (2009) *Clin. Cancer Res.* **15**, 3540–3549
47. Rabbani, S. A., Valentino, M. L., Arakelian, A., Ali, S., and Boschelli, F. (2010) *Mol. Cancer Ther.* **9**, 1147–1157